Atractylenolide I stimulates intestinal epithelial repair through polyamine-mediated Ca^{2+} signaling pathway

Hou-Pan Song , Xue-Qin Hou , Ru-Yi Li , Rong Yu , Xin Li , Sai-Nan Zhou , Hui-Yong Huang , Xiong Cai , Chi Zhou

PII: S0944-7113(17)30042-9
DOI: 10.1016/j.phymed.2017.03.001
Reference: PHYMED 52171

To appear in: *Phytomedicine*

Received date: 11 November 2016
Revised date: 11 February 2017
Accepted date: 2 March 2017

Please cite this article as: Hou-Pan Song , Xue-Qin Hou , Ru-Yi Li , Rong Yu , Xin Li , Sai-Nan Zhou , Hui-Yong Huang , Xiong Cai , Chi Zhou , Atractylenolide I stimulates intestinal epithelial repair through polyamine-mediated Ca^{2+} signaling pathway, *Phytomedicine* (2017), doi: 10.1016/j.phymed.2017.03.001

Atractylenolide I stimulates intestinal epithelial repair through polyamine-mediated Ca^{2+} signaling pathway

Hou-Pan Song[a, 1], Xue-Qin Hou[b, 1], Ru-Yi Li[a], Rong Yu[a], Xin Li[a], Sai-Nan Zhou[c], Hui-Yong Huang[a], Xiong Cai[a,d,*], Chi Zhou[e,**]

[a] *Hunan Provincial Key Laboratory of Diagnostic and Therapeutic Research in Chinese Medicine, Hunan University of Chinese Medicine, Changsha, Hunan 410208, China*

[b] *Institute of Pharmacology, Taishan Medical College, Taian, Shandong 271000, China*

[c] *The First Affiliated Hospital of Hunan University of Chinese Medicine, Changsha, Hunan 410007, China*

[d] *School of Chinese Materia Medica, Guangdong Pharmaceutical University, Guangzhou, Guangdong 510006, China*

[e] *The First Affiliated Hospital of Guangzhou University of Chinese Medicine, Guangzhou, Guangdong 510405, China*

[*] *Corresponding author:* School of Chinese Materia Medica, Guangdong Pharmaceutical University, 280 East Waihuan Road, Higher Education Mega Center, Panyu District, Guangzhou, Guangdong 510006, China.

Tel./fax: +86-20-3935-3163.

** *Corresponding author:* The First Affiliated Hospital of Guangzhou University of Chinese Medicine, 16 Jichang Road, Baiyun District, Guangzhou, Guangdong 510405, China. Tel./Fax: +86-20-3659-1211.

E-mail addresses: caix12@qq.com (X. Cai), chizhou12@qq.com (C. Zhou).

[1] These authors contributed equally to this work.

ABSTRACT

Background: An impairment of the integrity of the mucosal epithelial barrier can be observed in the course of various gastrointestinal diseases. The migration and proliferation of the intestinal epithelial (IEC-6) cells are essential repair modalities to the healing of mucosal ulcers and wounds. Atractylenolide I (AT-I), one of the major bioactive components in the rhizome of *Atractylodes macrocephala* Koidz. (AMR), possesses multiple pharmacological activities. This study was designed to investigate the therapeutic effects and the underlying molecular mechanisms of AT-I on gastrointestinal mucosal injury.

Methods: Scratch method with a gel-loading microtip was used to detect IEC-6 cell migration. The real-time cell analyzer (RTCA) system was adopted to evaluate IEC-6 cell proliferation. Intracellular polyamines content was determined using high performance liquid chromatography (HPLC). Flow cytometry was used to measure cytosolic free Ca^{2+} concentration ($[Ca^{2+}]_c$). mRNA and protein expression of TRPC1 and PLC-γ_1 were determined by real-time PCR and Western blotting assay respectively.

Results: Treatment of IEC-6 cells with AT-I promoted cell migration and proliferation, increased polyamines content, raised cytosolic free Ca^{2+} concentration ($[Ca^{2+}]_c$), and enhanced TRPC1 and PLC-γ_1 mRNA and protein expression. Depletion of cellular polyamines by DL-a-difluoromethylornithine (DFMO, an inhibitor of polyamine synthesis) suppressed cell migration and proliferation, decreased polyamines content, and reduced $[Ca^{2+}]_c$, which was paralleled by a decrease in TRPC1 and PLC-γ_1

mRNA and protein expression in IEC-6 cells. AT-I reversed the effects of DFMO on polyamines content, $[Ca^{2+}]_c$, TRPC1 and PLC-γ_1 mRNA and protein expression, and restored IEC-6 cell migration and proliferation to near normal levels.

Conclusion: Our data demonstrate that AT-I stimulates intestinal epithelial cell migration and proliferation via the polyamine-mediated Ca^{2+} signaling pathway. Therefore, AT-I may have the potential to be further developed as a promising therapeutic agent to treat diseases associated with gastrointestinal mucosal injury, such as inflammatory bowel disease and peptic ulcer.

Keywords: Atractylenolide I, Intestinal epithelial repair, Cell migration and proliferation, Polyamine, Cytosolic free Ca^{2+}

Abbreviations:

AT-I, Atractylenolide I; $[Ca^{2+}]_c$, Cytosolic free Ca^{2+} ; DFMO, DL-α-difluoromethylornithine; ODC, ornithine decarboxylase; PKC, protein kinase C; PLC, Phospholipase C; PUT, putrescine; SPD, spermidine; SPM, spermine; TRPC1, canonical transient receptor potential-1; TCM, traditional Chinese medicine.

Introduction

The epithelium of the gastrointestinal tract serves both as a physical barrier to microorganisms and as a border of the mucosal immune system. Sometimes the intestine suffers insults, due to very concentrated hydrochloric acid, reflux of bile salts, alcohol, drugs, and foodstuffs with relatively high or low temperatures, pH values, or osmolarity (Gao et al., 2013). Impairment of the gastrointestinal surface barrier is characteristic of several diseases and various pathological states, such as peptic and stress ulcers, inflammatory bowel disease (Crohn's disease and ulcerative colitis), nonsteroidal anti-inflammatory drug-induced mucosal bleeding, and mucosal injury or erosions induced by *Helicobacter pylori* infection (Rathor et al., 2014b).

The repair of impaired epithelial surface occurs at least through two mechanisms (Ray et al., 2003). The first one is the migration of adjacent wound epithelial cells to the damaged area, in order to cover it. This complex phenomenon includes well-established processes such as cytoskeleton reorganization, membrane protrusion formation, and focal adhesion to the extracellular matrix at the front edge and release of adhesion sites at the rear edge of migrating cells. The second mechanism includes replacement of lost cells through proliferation, which depends on DNA synthesis and begins 12 h after the start of healing. This second mechanism as well as the first one require polyamines such as spermidine (SPD), spermine (SPM) and their precursor putrescine (PUT) that either arise from diet (red meat and cheeses) and bacteria or are the extrusion products from villi of sloughed epithelial cells (Johnson and McCormack, 1999). The intracellular polyamine levels are primarily regulated by

ornithine decarboxylase (ODC) and α-Difluoromethylornithine (DFMO). ODC, a key enzyme of polyamine biosynthesis, catalyzes the first rate-limiting reaction in polyamine biosynthesis to produce PUT. PUT is then converted to SPD and SPM through the sequential addition of polyamine groups. DFMO is an irreversible restrainer of ODC and can specifically inhibit ODC activity, thus preventing the synthesis of cellular polyamines (Ray et al., 2005).

Cytosolic free Ca^{2+} ($[Ca^{2+}]_c$) concentration plays an important role in the regulation of cell migration and proliferation, and increased $[Ca^{2+}]_c$ promotes epithelial healing after wounding both *in vivo* and *in vitro* (Rao et al., 2007). In intestinal epithelial cells (IEC-6), $[Ca^{2+}]_c$ is increased mainly by Ca^{2+} release from intracellular Ca^{2+} stores (endoplasmic reticulum and sarcoplasmic reticulum) and Ca^{2+} influx through Ca^{2+} permeable channels in the plasma membrane (Rao et al., 2006). A number of studies have shown that the canonical transient receptor potential-1 (TRPC1) protein functions as a Ca^{2+}-permeable channel mediating capacitative Ca^{2+} entry which is activated by Ca^{2+} store depletion (Rao et al., 2006; Rao et al., 2010). Phospholipase C (PLC) is an important regulatory enzyme that catalyzes the hydrolysis of phosphatidylinositol (4, 5)-bisphosphate (PIP_2) to generate diacylglycerol (DAG) and inositol (1, 4, 5)-trisphosphate (IP_3). It is well known that DAG functions as a protein kinase C (PKC) activator and that IP_3 acts as a Ca^{2+}-mobilizing messenger, resulting in the release of Ca^{2+} from IP_3-sensitive intracellular Ca^{2+} stores and activation of Ca^{2+} influx via plasma membrane Ca^{2+}-permeable channels (Rao et al., 2007). Polyamines have been demonstrated to be

involved in the regulation of Ca^{2+} influx through the plasma membrane and Ca^{2+} release from intracellular Ca^{2+} stores. Moreover, polyamines are necessary for activation of TRPC1 channels and PLC-γ_1 expression in IEC-6 cells.

The rhizome of *Atractylodes macrocephala* Koidz. (AMR, Baizhu in Chinese, family Asteraceae), is one of the most popular medicinal herbs in traditional Chinese medicine (TCM) that has been widely used for thousands of years (Song et al., 2015). AMR is believed to possess action of, in terms of TCM, invigorating the function of the spleen and replenishing vital qi. TCM doctors mostly prescribe AMR for prevention and treatment of digestive disorders such as peptic ulcer and ulcerative colitis, which are mainly caused by gastrointestinal mucosal injury. Atractylenolide I (AT-I, 3,8aβ-Dimethyl-5-methylene-2,4,4aα,5,6,7,8,8a-octahydronaphtho[2,3-b]furan-2-one, Fig.1A) is one of the major bioactive components isolated from AMR and has drawn great attention due to its multiple therapeutic effects, such as antitumor (Liu et al., 2008; Wang et al., 2002; Yu et al., 2016), anti-inflammation (Endo et al., 1979; Wang et al., 2016), anti-atopic (Lim et al., 2012), and bone protective effects (Ha et al., 2013). However, the protective effects of AT-I on gastrointestinal mucosal injury have never been reported and the possible mechanisms underlying the gastrointestinal protection activity remains to be explored.

In this study, we tested the hypothesis that AT-I stimulated intestinal epithelial repair (cell migration and proliferation) after wounding through polyamine-mediated Ca^{2+} signaling by modulating TRPC1 and PLC-γ_1. First, we examined the effects of

AT-I on cell migration and proliferation, polyamines content, and $[Ca^{2+}]_c$ in IEC-6 cells after wounding. Second, we determined whether depletion of cellular polyamines by DFMO decreased the rate of cell migration and proliferation, polyamines content, and $[Ca^{2+}]_c$ in injured IEC-6 cells and further investigated whether AT-I restored cell migration and proliferation, polyamines content, and $[Ca^{2+}]_c$ in polyamine-deficient IEC-6 cells. Third, we determined whether AT-I increased TRPC1 and PLC-γ_1 expression in normal and polyamine-depleted IEC-6 cells.

Materials and methods

Materials

Dulbecco's Modified Eagle Medium (DMEM) and dialyzed fetal bovine serum (dFBS) were purchased from Gibco (Carlsbad, CA, USA). PUT, SPD, and SPM were obtained from Sigma-Aldrich (St. Louis, MO, USA). DL-α-difluoromethylornithine (DFMO) was purchased from Merck (Darmstadt, Germany). RNAiso Plus reagent, PrimeScript™ RT Master Mix, and SYBR Premix Ex Taq™ II were purchased from Takara (Shiga, Japan). The primary antibody, rabbit polyclonal anti-TRPC1 antibody (ab75322), rabbit polyclonal anti-phospholipase C gamma1 (PLC-γ_1) antibody (ab107455), mouse monoclonal anti-beta actin antibody (ab8226), the specific goat polyclonal secondary antibody to Rabbit IgG (ab7090), and goat polyclonal secondary antibody to mouse IgG (ab97040) were purchased from Abcam (Hong Kong, China). AT-I of 98% purity verified by the HPLC (Supplementary Fig. S1A and B) was

purchased from Guangzhou Haokai Reagent Co. Ltd. (Guangzhou, Guangdong, China). E-plate 16 was purchased from Roche (Basel, Switzerland). Other chemicals and biochemicals were obtained from Beyotime Biotechnology (Haimen, Jiangsu, China).

Cell culture

The IEC-6 cell line (CRL 1592) was obtained from the American Type Culture Collection (Manassas, VA, USA). IEC-6 cells were seeded in 6-well plates (6.25×10^4 cells/cm^2) and grown for 24 h in DMEM supplemented with 10% fetal bovine serum (FBS), 100 units/ml penicillin, and 100 μg/ml streptomycin. After 24 h, cells were treated with PUT (positive control, 10 μM), AT-I (5 and 10 μM), DFMO (5 mM), DFMO + PUT, or DFMO + AT-I for 8 h. In the following series of studies, we examined the effects of AT-I on cell migration and proliferation, polyamines content, $[Ca^{2+}]_c$, TRPC1 and PLC-γ_1 expression in normal and polyamine-depleted IEC-6 cells.

Cell migration assay

IEC-6 cells were treated as described in cell culture, and cell migration was measured as described previously (Ray et al., 2007a). In brief, plates were marked in the bottom by drawing five lines parallel to the diameter, and wounding of the monolayer was performed perpendicular to the marked line using a 1000 μl gel-loading microtip to initiate cell migration. Plates were washed with PBS to remove the damaged cells, and the area of migration was captured with an inverted phase contrast microscope (Olympus IX-71, Tokyo, Japan) at the intersection of the

marked lines and the wounded edge at 0 h (WW_0) and 8 h (WW_8), respectively. Cell migration was calculated as % wound area covered at 8 h according to the formula WW_0-WW_8/WW_0 by the NIH Image J software (version 1.58, Bethesda, MD, USA) (Ray et al., 2007a).

Cell proliferation assay

The proliferation of IEC-6 cells was determined by the Real-Time Cell Analyzer (RTCA) system (ACEA Biosciences, San Diego, CA, USA) according to the manufacturer's instruction. In details, 50 μl of cell-culture medium (DMEM supplemented with 10% FBS) was placed in each well of the E-plate 16. E-plate 16 was then connected to the RTCA system to obtain background impedance readings. Cells were trypsinized, resuspended, and seeded on E-plate 16 at a density of 10000/well with fresh medium to a final volume of 200 μl. Cell proliferation was monitored every 2 min by RTCA Software Package 1.2 until the end of the experiment (up to 72 h), and was measured as changes in impedance in the system. The assay system expressed impedance in arbitrary cell index (CI) units (Marlina et al., 2015).

HPLC analysis of cellular polyamines

The cellular polyamines PUT, SPD, and SPM were extracted from IEC-6 cells and homogenized with 5% perchloric acid. The perchloric supernatants were alkalinized by 2 mol/l NaOH solution, followed by the addition of 4% benzoyl chloride to form derivatives. The derivatives were separated and determined by Agilent 1200 reverse-phase high-performance liquid chromatography (RP-HPLC)

system equipped with auto-sampler, column oven, and ultraviolet (UV) detector. Data and spectrum were recorded and analyzed by the Agilent Chromatograpy Workstation (Palo Alto, CA, USA). Chromatographic separation was achieved with isocratic elution using a mobile phase composed of water (45%) and methanol (55%) at 1.0 ml/min flow rate. A Hypersil ODS C_{18} column (5 μm, 250 × 4.6 mm id) was used for separation and held at 25 °C, UV detection was carried out at the wavelength of 234 nm (Wong et al., 2016). The results were expressed as nM of polyamines *per* 1×10^6 cells.

Flow cytometry measurement of $[Ca^{2+}]_c$

Confluent cells were trypsinized, centrifuged, and resuspended to 4×10^6 cells/ml in PBS, the cultures were subsequently incubated with calcium sensing Fluo-3/AM at a final concentration of 5 μM for 30 min in the dark. Ca^{2+}-derived fluorescent signals were detected by a BD FACSCalibur flow cytometry (Franklin Lakes, NJ, USA) with an air-cooled 488-nm argon ion laser and CellQuest software. Forward scatter (FSC) and side scatter (SSC) were used to exclude cell debris from the analysis. FSC, SSC were displayed on a linear scale, and Fluo-3 fluorescence were displayed on a logarithmic scale (FL1) and recorded as mean fluorescence intensity (MFI) of the whole cell population. The excitation and emission were set at 495 nm and 525 nm, respectively (Hu et al., 2015). 1.0×10^4 cells were examined for each sample, and $[Ca^{2+}]_c$ was shown by MFI of the cells.

qRT-PCR analysis of gene expression

Total RNA was extracted using RNAiso Plus reagent. RNA integrity and purity

were measured immediately by gel electrophoresis and NanoDrop 2000 spectrophotometry (Thermo, MA, USA), respectively. RNAs (1 μg) were reverse transcribed into cDNA by PrimeScript^{TM} RT Master Mix according to the manufacturer's protocol. Quantitative real-time PCR was performed on the CFX96 system (Bio-Rad Laboratories, Hercules, CA, USA) in a 25 μl reaction volume containing 12.5 μl SYBR Premix Ex Taq™ II, 2 μl (100 nM) primers, 8.5 μl RNase free dH_2O, and 2 μl appropriately diluted cDNA template. Thermal cycling was initiated at 95 °C for 30 s and followed by 40 cycles of denaturation at 95 °C for 5 s and annealing at 60 °C for 30 s. Melt curves were obtained to ensure that nonspecific products were absent. Three independent reactions were repeated and the relative gene expression (RGE) was calculated by the comparative Ct method ($RGE = 2^{-\Delta\Delta CT}$) normalized to β-actin gene. The sequences of the primers used for qRT-PCR were: β-actin forward 5'-GGA GAT TAC TGC CCT GGC TCC TA-3' and β-actin reverse 5'-GAC TCA TCG TAC TCC TGC TTG CTG-3'; TRPC1 forward 5'-AGC CTC TTG ACA AAC GAG GA-3' and TRPC1 reverse 5'-ACC TGA CAT CTG TCC GAA CC-3'; PLC-γ_1 forward 5'-GAG GCC AAC CCT ATG CCA AC-3' and PLC-γ_1 reverse 5'-GGA TGA TGG GGC TCT TGG TAA-3'.

Western blotting analysis

For the Western blotting analysis of TRPC1 and PLC-γ_1, cells were washed twice with ice-cold PBS and harvested in cell lysis buffer supplemented with protease and phosphatase inhibitor cocktail tablets (Roche, Basel, Switzerland) by scraping with a rubber policeman. The amount of protein was determined by bicinchoninic acid (BCA)

protein assay reagent. Cell samples was boiled for 5 min and then subjected to electrophoresis on SDS-PAGE gels. After the transfer of protein onto polyvinylidene difluoride membranes, the membranes were incubated in 5% nonfat dry milk in TBST buffer for 1 h. Immunological evaluation was then performed overnight at 4 °C in 1% BSA-TBST buffer containing specific antibody against TRPC1 and PLC-γ_1 protein. The membranes were subsequently washed with TBST and incubated with the secondary antibodies conjugated with horseradish peroxidase (HRP) for 90 min at room temperature. Immunocomplexes were visualized using enhanced chemiluminescence detection reagent through the ChemiDoc XRS system (Bio-Rad Laboratories, Hercules, CA, USA). The densitometric intensity of bands on the images was determined by Image Lab software (Bio-Rad Laboratories, Hercules, CA, USA).

Statistical analysis

Data were expressed as the mean ± SD from six wells. qRT-PCR and western blot results were replicated three times. The significance of the difference between the means was determined by one-way and multiple analysis of variance (ANOVA). The level of significance was determined by using Dunnett's multiple-range test, and values of $P < 0.05$ were considered significant. Data were analyzed with the SPSS 19.0 software program.

Results

Influence of AT-I on IEC-6 cell migration after wounding

Fig. 1B shows phase-contrast images of wound areas at 0 and 8 h following scratching. Cells treated with AT-I (5 and 10 μM) or PUT (10 μM, reference drug) were shown to significantly cover the wound areas as compared with those of the control group (Fig.1B). PUT, 5 μM AT-I, and 10 μM AT-I given immediately after wounding increased the rate of cell migration by 45%, 43%, and 49%, respectively in control cells (Fig.1C). The results showed also that DFMO (a specific inhibitor of polyamine synthesis) significantly inhibited IEC-6 cell migration (Fig.1B). The area ratio of cells migrating in the DFMO-treated cells was decreased by 132% when counted at 8 h after wounding (Fig.1C). Supplementation of DFMO-containing medium with PUT, 5 μM AT-I or 10 μM AT-I restored the migration to the control levels (Fig.1C). These results suggest that AT-I stimulates IEC-6 cell migration in normal and polyamine-deficient conditions.

Insert Figure 1

Influence of AT-I on IEC-6 cell proliferation after wounding

As shown in Fig. 2A and B, in control cells (without DFMO), the value of cell index was remarkably increased after exposure to 5 and 10 μM AT-I (from 7.57 ± 0.39 to 8.69 ± 0.41 and 9.84 ± 0.46, respectively). In DFMO-treated cells, the basal level of cell index was significantly lower than that observed in control cells (from 7.57 ± 0.39 to 3.73 ± 0.51) (Fig. 2B); however, 5 and 10 μM AT-I significantly increased the cell index of IEC-6 cells grown in DFMO-containing medium and restored it to nearly control levels (Fig. 2B). These results indicate that AT-I could promote the proliferation of IEC-6 cells grown under either control or DFMO conditions.

Insert Figure 2

Influence of AT-I on cellular polyamines levels

The mean levels (nM/10^6 cells) of each polyamine and total polyamines were shown in Fig. 3 and Table 1. PUT levels of control increased by 31% when treated with 5 μM AT-I. SPD level of control treated with 5 and 10 μM AT-I was increased by 48% and 120%, respectively, and SPM level of control treated with 5 and 10 μM AT-I was increased by 42% and 116%, respectively. Exposure of monolayer cultures of IEC-6 to DFMO caused a dramatical reduction of polyamines levels. PUT, SPD, and SPM contents were reduced to 8%, 20%, and 22% of control, respectively, whereas pretreatment of the cells with AT-I completely reversed the inhibitory effect of DFMO on polyamines content. The levels of PUT, SPD, and SPM were all markedly increased when DFMO was given together with AT-I (5 and 10 μM). The total polyamines level of control increased by 41% and 120% respectively, following 5 and 10 μM AT-I treatment. In contrast, exposure to DFMO substantially decreased the total polyamines content. In the presence of DFMO, addition of AT-I to the cultures not only prevented the decreased level of total polyamines, but also restored total polyamines content to near normal level. These data indicate that AT-I has a significant effect on improving the content of polyamines in intestinal epithelial cells.

Insert Figure 3

Insert Table 1

Influence of AT-I on $[Ca^{2+}]_c$ in IEC-6 cells

In comparison with untreated control cells, we observed a pronounced increase

of fluo-3 fluorescence by about 61.6% and 105.4%, respectively, when IEC-6 cells were treated with 5 μM and 10 μM AT-I (Fig. 4A and B). DFMO imposed a decrease of fluorescence by about 136.7% in comparison with control cells. Addition of AT-I (5 and 10 μM) to the cultures in the presence of DFMO not only reversed the inhibitory effects of polyamine depletion on $[Ca^{2+}]_c$ but also restored $[Ca^{2+}]_c$ to normal levels (Fig. 4A and B). These results suggest that increased polyamines content caused by AT-I in IEC-6 cells could increase $[Ca^{2+}]_c$, which might play a critical role in the promotion of cell migration and proliferation after wounding.

Insert Figure 4

Influence of AT-I on TRPC1 and PLC-γ_1 mRNA expression

AT-I-treated IEC-6 cells displayed a substantial increase in the levels of TRPC1 and PLC-γ_1 mRNA (Fig. 5A and B). Levels of TRPC1 and PLC-γ_1 mRNA in cells treated with 5 μM AT-I were increased by 89% and 86%, respectively, and levels of TRPC1 and PLC-γ_1 mRNA were increased by 106% and 101%, respectively, in cells exposed to 10 μM AT-I. Inhibition of polyamine biosynthesis by DFMO was associated with decreases in TRPC1 and PLC-γ_1 mRNA expression. In DFMO-treated cells, levels of TRPC1 and PLC-γ_1 mRNA were decreased by 146% and 140%, respectively. Supplementation with AT-I (5 and 10 μM) reversed the DFMO-triggered changes in TRPC1 and PLC-γ_1 mRNA expression, levels of TRPC1 and PLC-γ_1 mRNA in cells exposed to DFMO plus AT-I were similar to those of control cells.

Insert Figure 5

Influence of AT-I on TRPC1 and PLC-γ_1 protein expression

Consistent with the augmenting effect on mRNA expression, administration of AT-I also increased TRPC1 and PLC-γ_1 protein expression in control and polyamine-deficient cells. As shown in Fig. 6A, B, and C, the protein levels of TRPC1 and PLC-γ_1 of the cells treated with 5 μM AT-I were increased by 79% and 87%, respectively, when compared with control cells. IEC-6 cells treated with 10 μM AT-I also displayed a substantial increase in the levels of TRPC1 and PLC-γ_1 protein, which were both approximately twice those of the control cells. Inhibition of polyamine biosynthesis by DFMO significantly decreased TRPC1 and PLC-γ_1 protein expression, the protein levels of TRPC1 and PLC-γ_1 in DFMO-treated cells were decreased by 188% and 253%, respectively. Addition of AT-I (5 and 10 μM) given together with DFMO restored TRPC1 and PLC-γ_1 protein to near normal levels.

Insert Figure 6

Discussion

The gastrointestinal mucosal epithelium represents an important barrier between a large number of noxious and immunogenic substances present in the lumen of the gut and the organism. Impairment of the gastrointestinal surface barrier is observed in the course of various diseases, such as celiac disease, peptic ulcer, and inflammatory bowel diseases. This pathological process may lead to increased penetration and absorption of toxic and immunogenic components into the host resulting in inflammation, uncontrolled immune response, and an imbalance of the homeostasis of the body. Impairment of the gastrointestinal epithelium can result from food products,

ionizing radiation, chemicals (alcohol), chemotherapeutic agents (antibiotics, hormones, or other drugs), or mechanical forces (stretching), and immediate repair is required to restore the function of mucosal epithelial barrier against luminal antigens (Vaidya et al., 2005). Observations over the past several years have demonstrated that the mucosa of the gastrointestinal tract is one of the fastest growing and rapidly turning-over tissues in the body, and gastrointestinal repair is a continuous process that can be divided into two phases, namely, cell migration and proliferation.

The regulation of the migration and proliferation of intestinal epithelial cells in response to injury is crucial for the preservation of gastrointestinal mucosal integrity under physiological and pathological conditions. This regulation is unique because it not only depends on normal blood-borne substances but is also influenced by trophic hormones secreted from the mucosa and by other factors present within the digestive tract (Ray and Johnson, 2014). Polyamines are known to play a critical role in the regulation of migration and proliferation of intestinal epithelial cells. The polyamines PUT, SPD, and SPM are found virtually in all eukaryotic cells. The activity of polyamines is closely related to their positive charges. PUT, SPD, and SPM are organic, aliphatic, cationic amines, with pK values above 9. Under physiological pH, they strongly bind to negatively charged macromolecules such as RNA, DNA, and proteins to regulate diverse biological effects (Ray et al., 2011). Polyamines synthesis is highly regulated and primarily relies on the activity of ODC that catalyses the decarboxylation of ornithine to form the diamine PUT. PUT is then in turn converted to SPD and SPM by the addition of a propylamine group. DFMO is a suicide inhibitor

of ODC that prevents the formation of polyamines. Following DFMO treatment, intracellular PUT is depleted within 6 h, SPD within 24 h, and SPM to 50% within 96 h.

A large body of research have demonstrated that IEC-6 cells that are polyamine deficient fail to migrate normally during the early phase of restitution, and polyamine depletion decreases the rate of IEC-6 cell proliferation by G1 cell cycle arrest (Rathor et al., 2014a; Ray et al., 2011; Ray et al., 2003; Ray et al., 2007b; Wang et al., 2000; Zhang et al., 2014). In the present study, we found that AT-I significantly increased the migration (Fig. 1) and proliferation (Fig. 2) of cells grown under control conditions. Polyamine depletion by DFMO caused delayed migration and proliferation of IEC-6 cells, while addition of AT-I together with DFMO restored migration (Fig. 1) and proliferation (Fig. 2) to the levels of control, suggesting that the observed effects of AT-I was associated with its regulation in increasing intracellular polyamines content. We then further determined the effect of AT-I on intracellular polyamines content in control (without DFMO) and polyamine depleted IEC-6 cells. The results shown in Fig. 3 and Table 1 confirmed that AT-I indeed enhances the polyamines levels during IEC-6 cell migration and proliferation. Exposure of IEC-6 cells to 5 or 10 μM AT-I for 24 h, which notably increased the total cellular polyamines levels. Polyamine depletion by DFMO significantly decreased the total polyamines content, whereas AT-I given together with DFMO completely abolished the inhibitory effect of DFMO on polyamines synthesis.

Several lines of research have demonstrated that cellular polyamines stimulate

epithelial cell migration and proliferation during wound healing process primarily by modulating the cytosolic free Ca^{2+} concentration ($[Ca^{2+}]_c$) (Rao et al., 2001; Rao et al., 2002). Other reports further proved that polyamines regulate $[Ca^{2+}]_c$ by altering TRPC1 and PLC-γ_1 activity, and that polyamine-mediated TRPC1 and PLC-γ_1 expression plays an important role in intestinal epithelial cell migration and proliferation after wounding (Rao et al., 2007; Rao et al., 2008; Rao et al., 2006; Rao et al., 2010). Our findings clearly showed that the increase of cellular polyamines caused by AT-I treatment remarkably elevated $[Ca^{2+}]_c$ (Fig. 4). Depletion of intracellular polyamines by DFMO markedly reduced $[Ca^{2+}]_c$ in IEC-6 cells, while exposure of IEC-6 cells to AT-I completely reversed the restrained effects of polyamine depletion on $[Ca^{2+}]_c$ elicited by DFMO (Fig. 4). To provide insight into the molecular basis for the enhancement of $[Ca^{2+}]_c$ induced by AT-I, the results presented in Fig. 5 indicate that levels of TRPC1 and PLC-γ_1 mRNA increased significantly in cells treated with AT-I for 24 h, and TRPC1 and PLC-γ_1 mRNA levels decreased significantly in cells treated with DFMO. However, this inhibition of TRPC1 and PLC-γ_1 mRNA expression in DFMO-treated cells was completely prevented by AT-I treatment (Fig. 5). Consistent with the augmenting effect on mRNA expression, administration of AT-I also increased TRPC1 and PLC-γ_1 protein expression in control and polyamine-deficient IEC-6 cells (Fig. 6).

AMR, one of the traditional Chinese herbal drugs listed in Chinese Pharmacopoeia, has remarkable effects on digestive system diseases, such as peptic ulcer, diarrhea, etc. AT-I, an active compound isolated from AMR, has been shown to

exhibit a wide variety of biological and pharmacological activities. Zhang et al. showed that AT-I protected mice acute lung injury induced by LPS via inhibition of TLR4 expression and NF-κB activation (Zhang et al., 2015). Ma et al. reported that AT-I attenuated gastric cancer stem cell traits partly through inactivating Notch1, leading to reducing the expressions of its downstream target Hes1, Hey1 and CD44 *in vitro* (Ma et al., 2014). In a recent study, Yu et al. reported that AT-1 showed dose-dependent anti-tumor effects on human bladder cancer cells through arresting cell cycle, inducing apoptosis, and inhibition of PI3K/Akt/mTOR signaling pathway (Yu et al., 2016). The findings reported here clearly show that AT-I stimulated intestinal epithelial cell migration and proliferation via polyamine-mediated Ca^{2+} signaling pathway. Thus, AT-I is a valuable natural drug which may play an important role in the treatment of diseases caused by gastrointestinal mucosal injury individually or in combination with other pharmaceuticals. However, further *in vivo* studies are needed to be carried out to intensively dissect the molecular mechanism underlying the therapeutic effect of AT-I on gastrointestinal mucosal injury.

Conclusions

In summary, our results indicate that polyamine-mediated Ca^{2+} signaling pathway is involved in AT-I-afforded intestinal epithelial cell migration and proliferation. Treatment of IEC-6 cells with AT-I promotes cell migration and proliferation, increases polyamines content, raises $[Ca^{2+}]_c$, and enhances TRPC1 and PLC-γ_1 mRNA and protein expression. Depletion of cellular polyamines by DFMO suppresses cell migration and proliferation, decreases polyamines content, and

reduces $[Ca^{2+}]_c$, which is paralleled by a decrease in TRPC1 and PLC-γ_1 mRNA and protein expression in IEC-6 cells. AT-I reverses the effects of DFMO on polyamines content, $[Ca^{2+}]_c$, TRPC1 and PLC-γ_1 mRNA and protein expression, and restores cell migration and proliferation to near normal levels. Thereby, AT-I may be developed as a potential therapeutic agent to treat diseases associated with gastrointestinal mucosal injury by further investigation.

Acknowledgments

This work was funded by grants from the National Natural Science Foundation of China (Grant no. 81373540), the China Postdoctoral Science Foundation (Grant no. 2016M600632), the Outstanding Youth Project of Hunan Department of Education (Grant no. 15B179), the Doctoral Research Project of Hunan University of Chinese Medicine (Grant no. 2014-1001-017), the Open Fund Project of State Key Subject of Diagnostics in Chinese Medicine of Hunan University of Chinese Medicine (Grant nos. 2015ZYZD19, 2015ZYZD16), and was supported by 225 High-level Medical Professional Training Program of Hunan Health and Family Planning Commission, and 2015 Program for Innovative Research Team of Hunan University of Chinese Medicine.

Conflicts of interest

The authors declare no potential conflict of interest.

References

Endo, K., Taguchi, T., Taguchi, F., Hikino, H., Yamahara, J., Fujimura, H., 1979. Antiinflammatory principles of Atractylodes rhizomes. Chem. Pharm. Bull. 27, 2954-2958.

Gao, J.H., Guo, L.J., Huang, Z.Y., Rao, J.N., Tang, C.W., 2013. Roles of cellular polyamines in mucosal healing in the gastrointestinal tract. J. Physiol. Pharmacol. 64, 681-693.

Ha, H., An, H., Shim, K.S., Kim, T., Lee, K.J., Hwang, Y.H., Ma, J.Y., 2013. Ethanol extract of Atractylodes macrocephala protects bone loss by inhibiting osteoclast differentiation. Molecules 18, 7376-7388.

Hu, X.L., Gao, L.Y., Niu, Y.X., Tian, X., Wang, J., Meng, W.H., Zhang, Q., Cui, C., Han, L., Zhao, Q.C., 2015. Neuroprotection by Kukoamine A against oxidative stress may involve N-methyl-D-aspartate receptors. Biochim. Biophys. Acta. 1850, 287-298.

Johnson, L.R., McCormack, S.A., 1999. Healing of gastrointestinal mucosa: involvement of polyamines. News Physiol. Sci. 14, 12-17.

Lim, H., Lee, J.H., Kim, J., Kim, Y.S., Kim, H.P., 2012. Effects of the rhizomes of Atractylodes japonica and atractylenolide I on allergic response and experimental atopic dermatitis. Arch. Pharm. Res. 35, 2007-2012.

Liu, Y., Jia, Z., Dong, L., Wang, R., Qiu, G., 2008. A randomized pilot study of atractylenolide I on gastric cancer cachexia patients. Evid. Based Complement. Alternat. Med. 5, 337-344.

Ma, L., Mao, R., Shen, K., Zheng, Y., Li, Y., Liu, J., Ni, L., 2014. Atractylenolide I-mediated Notch pathway inhibition attenuates gastric cancer stem cell traits. Biochem Biophys Res Commun 450, 353-359.

Marlina, S., Shu, M.H., AbuBakar, S., Zandi, K., 2015. Development of a Real-Time Cell Analysing (RTCA) method as a fast and accurate screen for the selection of chikungunya virus replication inhibitors. Parasit Vectors 8, 579.

Rao, J.N., Li, L., Golovina, V.A., Platoshyn, O., Strauch, E.D., Yuan, J.X., Wang, J.Y., 2001. Ca2+-RhoA signaling pathway required for polyamine-dependent intestinal epithelial cell migration. Am. J. Physiol. Cell Physiol. 280, C993-1007.

Rao, J.N., Liu, L., Zou, T., Marasa, B.S., Boneva, D., Wang, S.R., Malone, D.L., Turner, D.J., Wang, J.Y., 2007. Polyamines are required for phospholipase C-gamma1 expression

promoting intestinal epithelial restitution after wounding. Am. J. Physiol. Gastrointest. Liver. Physiol. 292, G335-343.

Rao, J.N., Liu, S.V., Zou, T., Liu, L., Xiao, L., Zhang, X., Bellavance, E., Yuan, J.X., Wang, J.Y., 2008. Rac1 promotes intestinal epithelial restitution by increasing Ca2+ influx through interaction with phospholipase C-(gamma)1 after wounding. Am. J. Physiol. Cell Physiol. 295, C1499-1509.

Rao, J.N., Platoshyn, O., Golovina, V.A., Liu, L., Zou, T., Marasa, B.S., Turner, D.J., Yuan, J.X., Wang, J.Y., 2006. TRPC1 functions as a store-operated Ca2+ channel in intestinal epithelial cells and regulates early mucosal restitution after wounding. Am. J. Physiol. Gastrointest. Liver. Physiol. 290, G782-792.

Rao, J.N., Platoshyn, O., Li, L., Guo, X., Golovina, V.A., Yuan, J.X., Wang, J.Y., 2002. Activation of K(+) channels and increased migration of differentiated intestinal epithelial cells after wounding. Am. J. Physiol. Cell Physiol. 282, C885-898.

Rao, J.N., Rathor, N., Zou, T., Liu, L., Xiao, L., Yu, T.X., Cui, Y.H., Wang, J.Y., 2010. STIM1 translocation to the plasma membrane enhances intestinal epithelial restitution by inducing TRPC1-mediated Ca2+ signaling after wounding. Am. J. Physiol. Cell Physiol. 299, C579-588.

Rathor, N., Chung, H.K., Wang, S.R., Wang, J.Y., Turner, D.J., Rao, J.N., 2014a. Caveolin-1 enhances rapid mucosal restitution by activating TRPC1-mediated Ca2+ signaling. Physiol. Rep. 2, e12193.

Rathor, N., Zhuang, R., Wang, J.Y., Donahue, J.M., Turner, D.J., Rao, J.N., 2014b. Src-mediated caveolin-1 phosphorylation regulates intestinal epithelial restitution by altering Ca(2+) influx after wounding. Am. J. Physiol. Gastrointest. Liver Physiol. 306, G650-658.

Ray, R.M., Bavaria, M.N., Bhattacharya, S., Johnson, L.R., 2011. Activation of Dbl restores migration in polyamine-depleted intestinal epithelial cells via Rho-GTPases. Am. J. Physiol. Gastrointest. Liver Physiol. 300, G988-997.

Ray, R.M., Bhattacharya, S., Johnson, L.R., 2005. Protein phosphatase 2A regulates apoptosis in intestinal epithelial cells. J. Biol. Chem. 280, 31091-31100.

Ray, R.M., Guo, H., Patel, M., Jin, S., Bhattacharya, S., Johnson, L.R., 2007a. Role of myosin regulatory light chain and Rac1 in the migration of polyamine-depleted intestinal epithelial

cells. Am. J. Physiol. Gastrointest. Liver Physiol. 292, G983-995.

Ray, R.M., Johnson, L.R., 2014. Regulation of intestinal mucosal growth by amino acids. Amino Acids 46, 565-573.

Ray, R.M., McCormack, S.A., Covington, C., Viar, M.J., Zheng, Y., Johnson, L.R., 2003. The requirement for polyamines for intestinal epithelial cell migration is mediated through Rac1. J. Biol. Chem. 278, 13039-13046.

Ray, R.M., Vaidya, R.J., Johnson, L.R., 2007b. MEK/ERK regulates adherens junctions and migration through Rac1. Cell Motil Cytoskeleton 64, 143-156.

Song, H.P., Li, R.L., Zhou, C., Cai, X., Huang, H.Y., 2015. Atractylodes macrocephala Koidz stimulates intestinal epithelial cell migration through a polyamine dependent mechanism. J. Ethnopharmacol. 159, 23-35.

Vaidya, R.J., Ray, R.M., Johnson, L.R., 2005. MEK1 restores migration of polyamine-depleted cells by retention and activation of Rac1 in the cytoplasm. Am. J. Physiol. Cell Physiol. 288, C350-359.

Wang, A., Xiao, Z., Zhou, L., Zhang, J., Li, X., He, Q., 2016. The protective effect of atractylenolide I on systemic inflammation in the mouse model of sepsis created by cecal ligation and puncture. Pharmaceutical biology 54, 146-150.

Wang, C.C., Chen, L.G., Yang, L.L., 2002. Cytotoxic activity of sesquiterpenoids from Atractylodes ovata on leukemia cell lines. Planta medica 68, 204-208.

Wang, J.Y., Wang, J., Golovina, V.A., Li, L., Platoshyn, O., Yuan, J.X., 2000. Role of K(+) channel expression in polyamine-dependent intestinal epithelial cell migration. Am. J. Physiol. Cell Physiol. 278, C303-314.

Wong, J.M., Malec, P.A., Mabrouk, O.S., Ro, J., Dus, M., Kennedy, R.T., 2016. Benzoyl chloride derivatization with liquid chromatography-mass spectrometry for targeted metabolomics of neurochemicals in biological samples. J. Chromatogr. A 1446, 78-90.

Yu, R., Yu, B.X., Chen, J.F., Lv, X.Y., Yan, Z.J., Cheng, Y., Ma, Q., 2016. Anti-tumor effects of Atractylenolide I on bladder cancer cells. J. Exp. Clin. cancer Res. 35, 40.

Zhang, J.L., Huang, W.M., Zeng, Q.Y., 2015. Atractylenolide I protects mice from lipopolysaccharide-induced acute lung injury. Eur. J. Pharmacol. 765, 94-99.

Zhang, X., Zou, T., Rao, J.N., Liu, L., Xiao, L., Wang, P.Y., Cui, Y.H., Gorospe, M., Wang, J.Y.,

2014. Stabilization of XIAP mRNA through the RNA binding protein HuR regulated by cellular polyamines. Nucleic Acids Res. 42, 4143.

Figure legends

Fig. 1. Effect of AT-I on IEC-6 cell migration in normal and polyamine-deficient conditions. (**A**) chemical structure of AT-I. (**B**) Representative images showing changes in cell migration (scale bar = 10 μm). (**C**) Quantitative analysis of migration showing wound area covered as compared with initial scratch size. Values are expressed as the means ± SD (n = 6). $^{**}P < 0.01$, compared with Control. $^{\#\#}P < 0.01$, compared with DFMO.

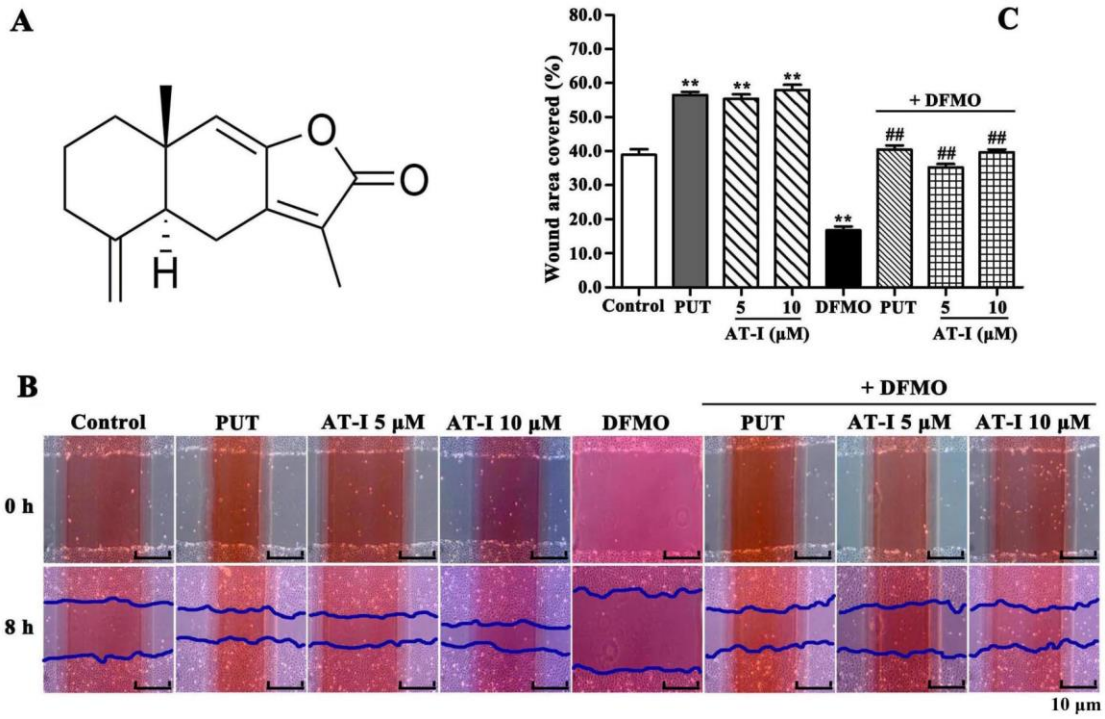

Fig. 2. Effect of AT-I on IEC-6 cell proliferation after wounding. (**A**) Representative recordings showing changes in cell index. (B) Summarized data showing cell index in IEC-6 cells . Data are expressed as the means ± SD (n = 6). $^{*}P < 0.05$, $^{**}P < 0.01$, compared with Control. $^{\#}P < 0.05$, $^{\#\#}P < 0.01$, compared with DFMO.

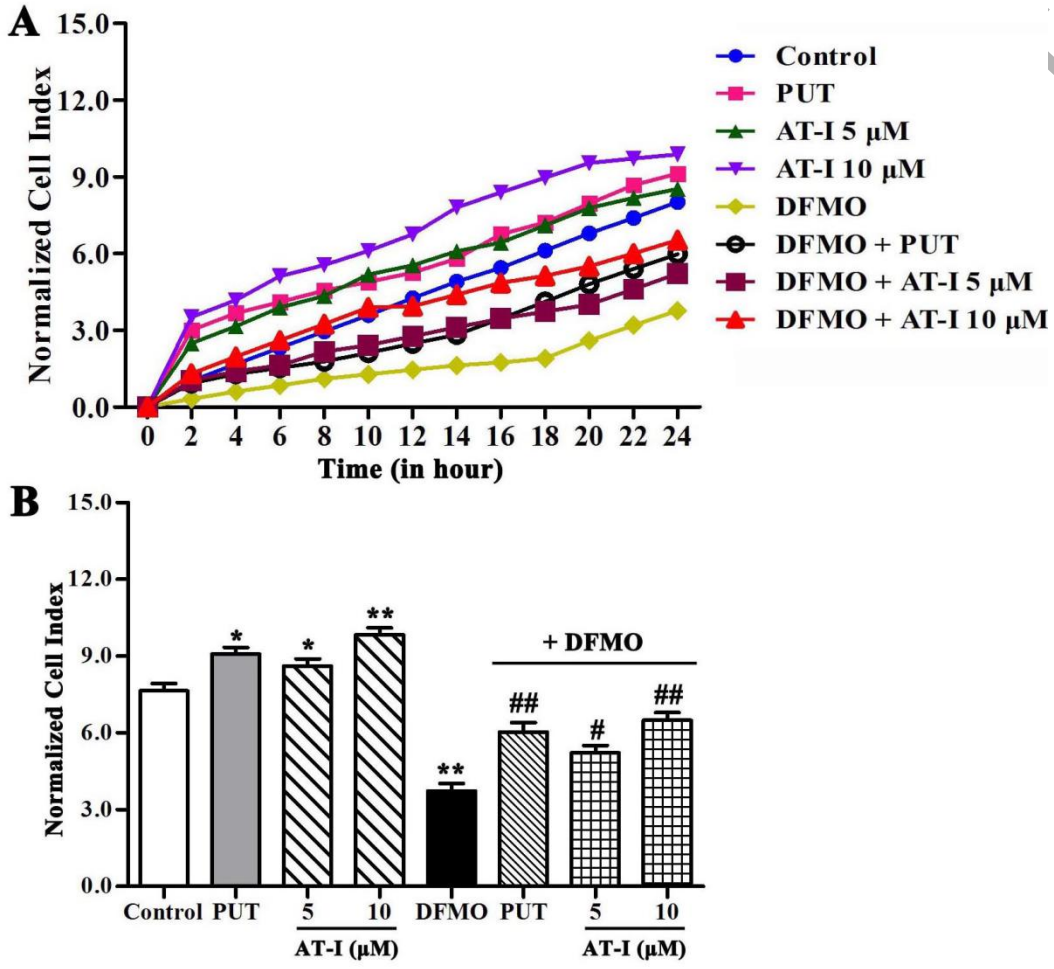

Fig. 3. The representative HPLC chromatograms of benzoylated polyamines from IEC-6 cells during wound healing process. Peaks: 1 = PUT, 2 = SPD, 3 = SPM.

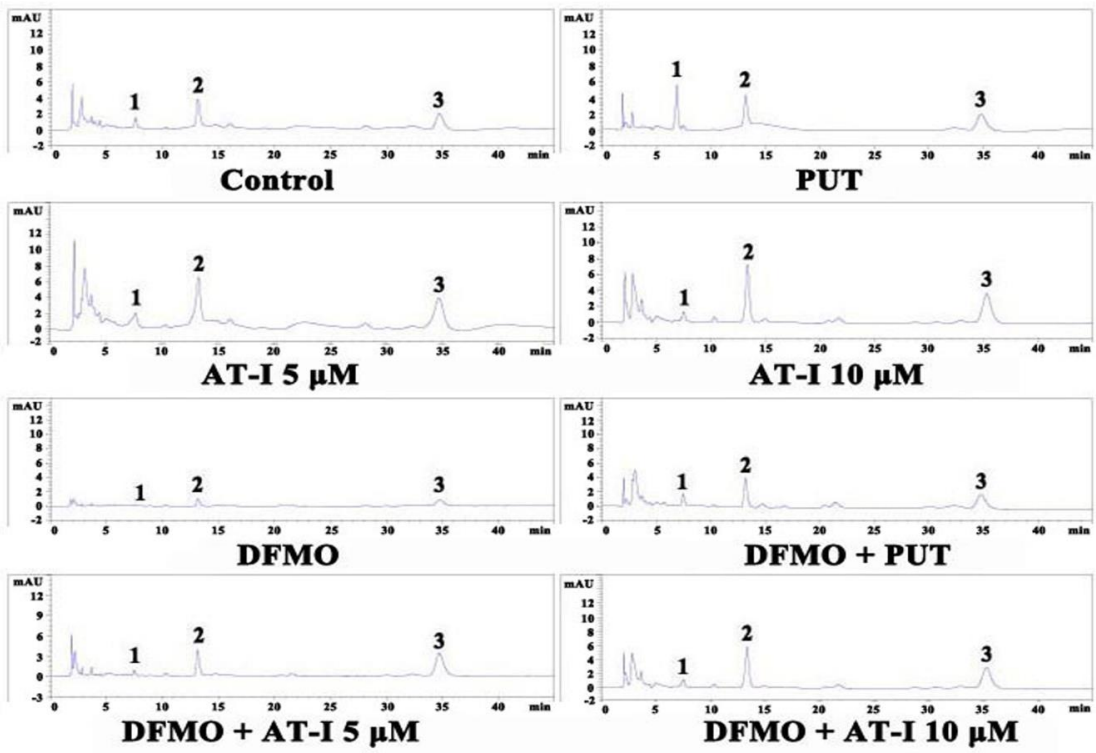

Fig. 4. Effect of AT-I on $[Ca^{2+}]_c$ during intestinal epithelial cell wound healing process. (**A**) Representative flow cytometric fluorescence images of IEC-6 cells. (**B**) Bar graphs displayed quantitative analysis of $[Ca^{2+}]_c$. Values of fluorescence intensity are presented as the means ± SD (n = 6). $^{**}P < 0.01$, compared with Control. $^{\#\#}P < 0.01$, compared with DFMO.

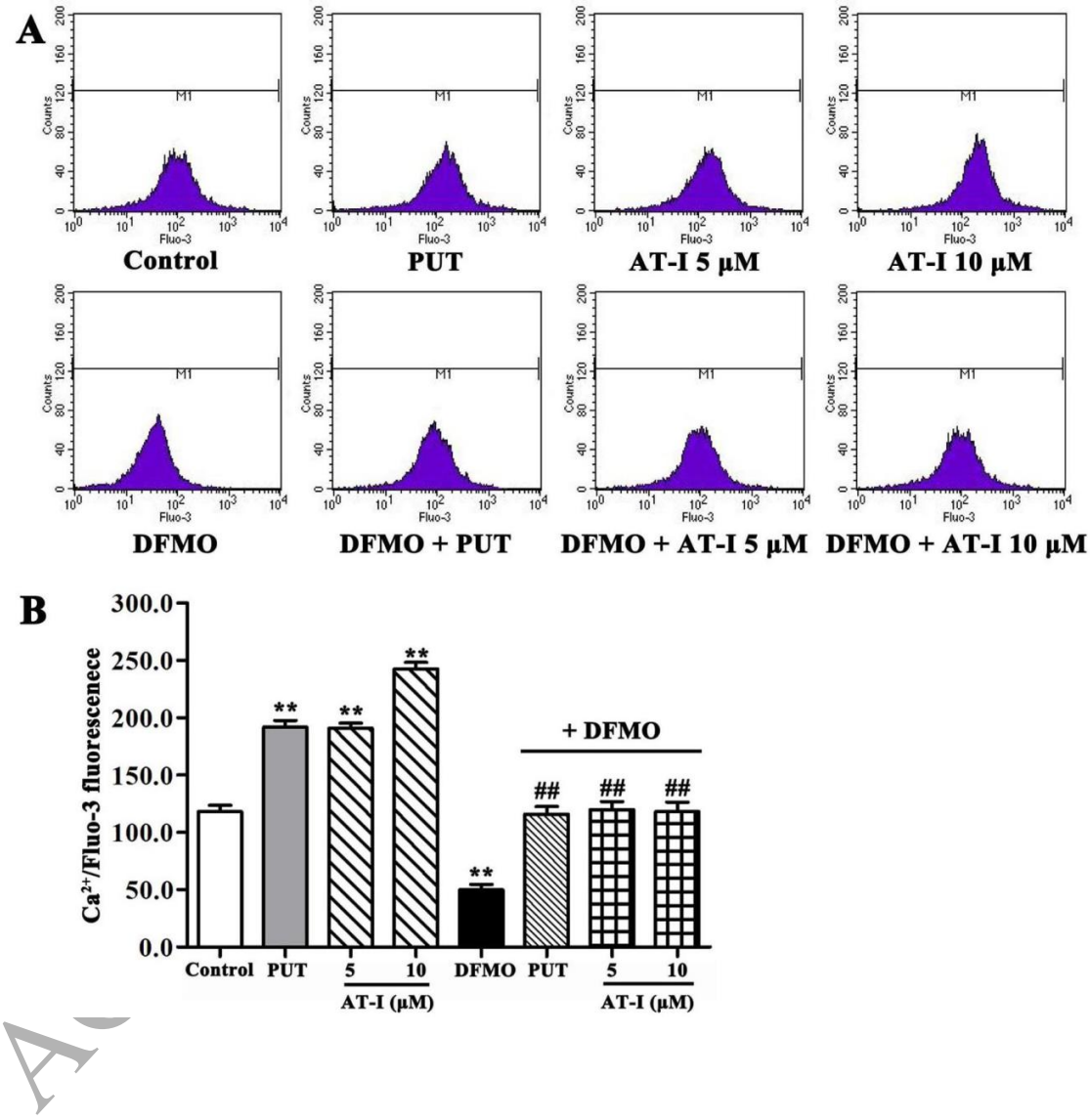

Fig. 5. Effect of AT-I on mRNA expression of TRPC1 (A) and PLC-γ_1 (B) in IEC-6 cells. Values are expressed as the means ± SD of data from three separate experiments. $^{**}P < 0.01$, compared with Control. $^{\#\#}P < 0.01$, compared with DFMO.

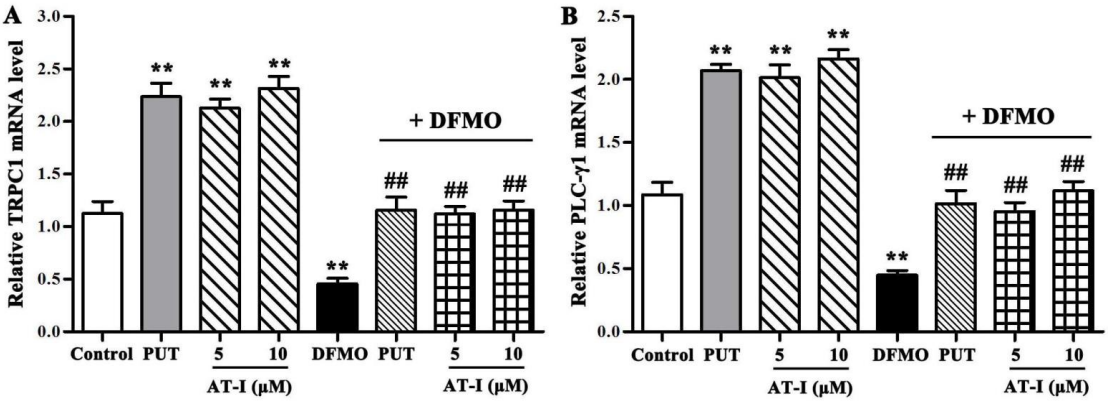

Fig. 6. Effect of AT-I on TRPC1 and PLC-γ_1 protein expression in IEC-6 cells. (**A**) representative immunoblots of TRPC1 and PLC-γ_1 in IEC-6 cells. (**B-C**) densitometric analysis of TRPC1 and PLC-γ_1 levels from the blots. Values are expressed as the means ± SD of data from three separate experiments. $^{**}P < 0.01$, compared with Control. $^{\#\#}P < 0.01$, compared with DFMO.

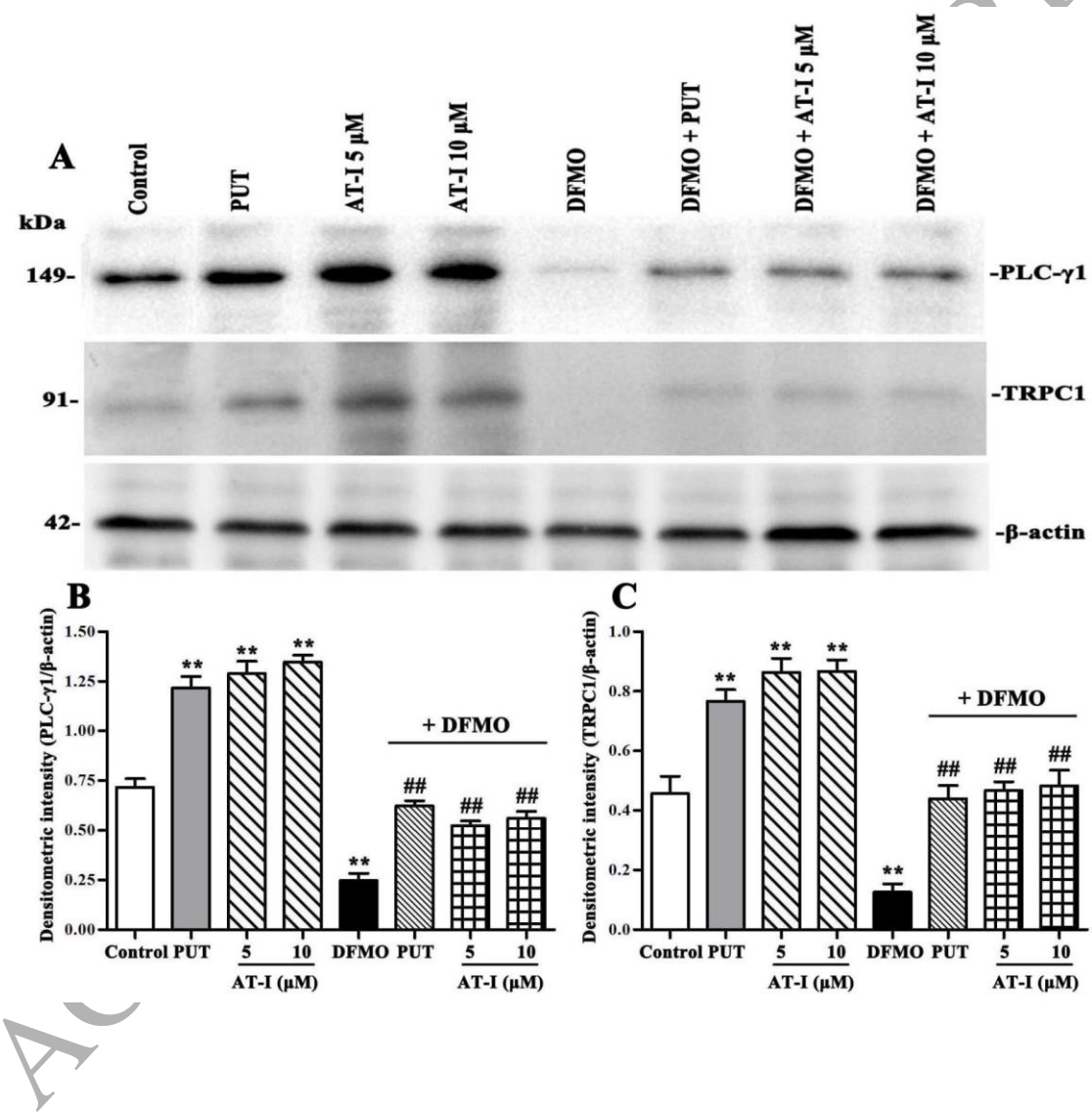

Table legend

Table 1. Amounts of polyamines in IEC-6 cells during wound healing process

(mean ± SD, n = 6)

Treatment	Polyamines level (nmol/10^6 cells)			
	PUT	SPD	SPM	total
Control	8.05 ± 0.83	15.91 ± 1.49	41.27 ± 3.63	65.15 ± 3.44
PUT (10 μmol/l)	35.12 ± 2.68**	18.95 ± 1.91**	52.69 ± 3.75**	106.92 ± 3.64**
AT-I (5 μmol/l)	10.53 ± 0.38*	23.6 ± 3.01**	58.50 ± 4.22**	91.63 ± 3.98**
AT-I (10 μmol/l)	8.42 ± 1.13	35.04 ± 3.68**	89.30 ± 6.28**	132.16 ± 6.15**
DFMO (2.5 mmol/l)	0.68 ± 0.12**	3.21 ± 0.37**	8.92 ± 1.03**	12.88 ± 0.92**
DFMO + PUT	8.37 ± 0.88$^{\#\#}$	18.44 ± 2.32$^{\#\#}$	43.2 ± 4.13$^{\#\#}$	70.01 ± 4.03$^{\#\#}$
DFMO + AT-I 5 μmol/l	1.84 ± 0.17$^{\#\#}$	15.26 ± 1.63$^{\#\#}$	42.45 ± 2.86$^{\#\#}$	59.24 ± 2.77$^{\#\#}$
DFMO + AT-I 10 μmol/l	4.35 ± 0.95$^{\#\#}$	26.04 ± 1.54$^{\#\#}$	52.13 ± 3.79$^{\#\#}$	82.43 ± 4.43$^{\#\#}$

$^{*}P < 0.05$, $^{**}P < 0.01$, compared with Control; $^{\#\#}P < 0.01$, compared with DFMO.

Graphical abstract